Ocean ventilation controls the contrasting anthropogenic CO_2 uptake rates between the western and eastern South Atlantic Ocean basins

Hui Gao (huigao@udel.edu) **and Wei-Jun Cai *** (wcai@udel.edu)

School of Marine Science and Policy, University of Delaware, Newark, Delaware, USA.

Based on Gao et al. 2022. GBC, https://doi.org/10.1029/2021GB007265

Introduction

Oceanic uptake of atmospheric carbon dioxide (CO_2) is a key part of the global CO_2 budget. Human activities have increased the partial pressure of CO_2 (pCO_2) in the atmosphere from ~280 ppm before the Industrial Revolution to well above 400 ppm at present. The ocean has absorbed 25-30% of the anthropogenic CO_2 from the atmosphere and has played an essential role in regulating atmospheric CO_2 concentration and our planet's climate conditions.

The Mid-Atlantic Ridge separates the South Atlantic Ocean into the western and eastern basin, with different geomorphology and circulation, and thus, anthropogenic CO_2 or carbon (C_{anth}) uptake and storage rates may have both a meridional and zonal gradient.

Study Region and Methods

The study region focuses on the South Atlantic Ocean from 60°W to 20°E (Figure 1a). The Mid-Atlantic Ridge separates the eastern and western Atlantic basins and rises to a depth of ~2000 m. Meridional transects A13.5 and A16S (Figure 1a) are located, on the east and west sides of the Mid-Atlantic Ridge, respectively. In addition, there is a zonal section A10 along 30°S.

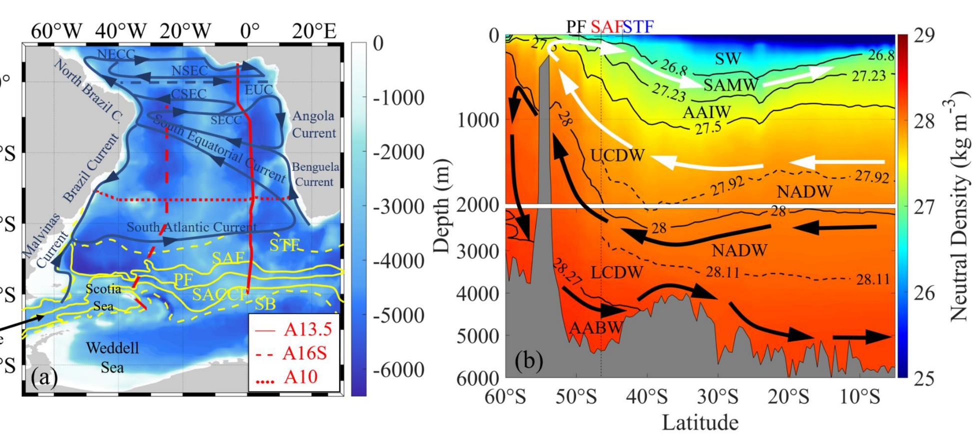

Figure 1. (a) Map of South Atlantic. (b) Water masses in the South Atlantic Ocean, and schematic diagram of the upper cell (white arrows) and the lower cell (dark arrows) of the Atlantic meridional overturning circulation (AMOC) in the South Atlantic

Applying the specific eMLR method:

Step1 divide water column into 5 layers based on water masses and neutral density

Step 2 compute C*

$$C^* = DIC - r_{C:O_2}O_2 - \frac{1}{2}\left(\mathrm{TA} + r_{N:O_2}O_2\right)$$

Step 3 build regression equitions

selected 11 best combinations of regression from more than 100 combinations

$$C^*(t) = A + B \cdot P_1 + C \cdot P_2 + D \cdot P_3 + \cdots + Residuals$$

Step 4 anthropogenic CO_2 changes

$$\Delta C_{anth}(t_2 - t_1) = (A_2 - A_1) + (B_2 - B_1) \cdot P_1 + (C_2 - C_1) \cdot P_2 + (D_2 - D_1) \cdot P_3 + \cdots$$

Results and Discussion: 1. Water Properties

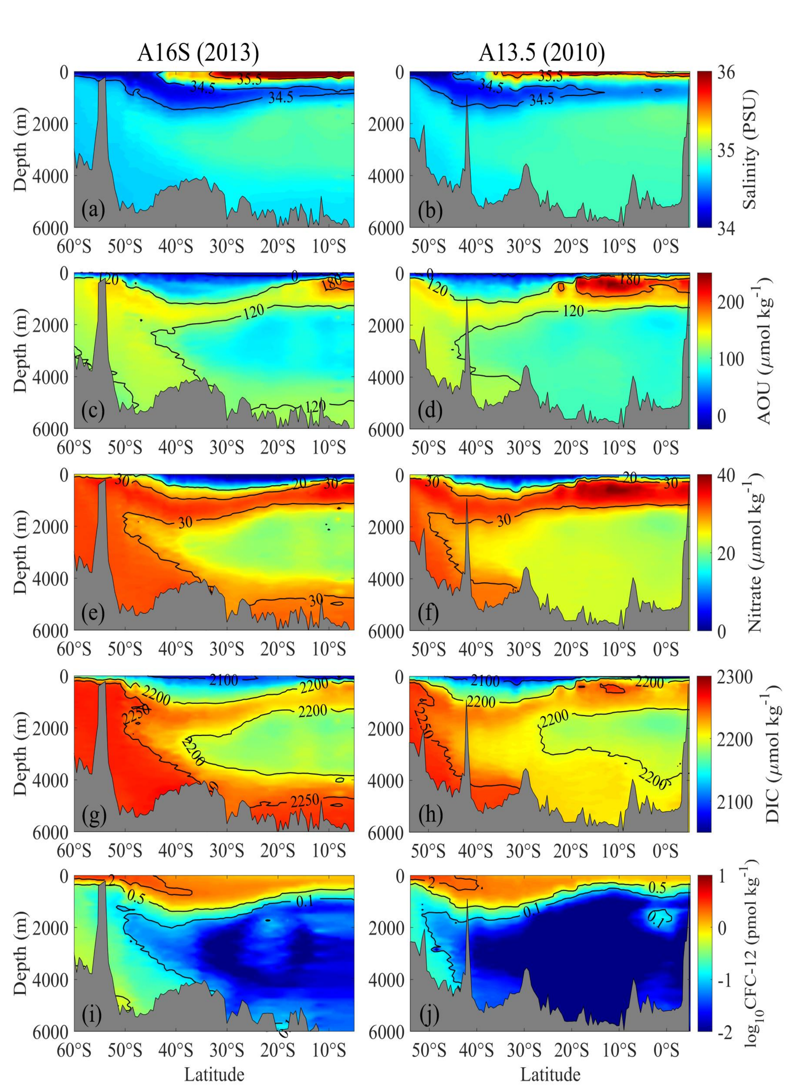

Figure 2. Vertical distribution of (a) & (b) salinity, (c) & (d) AOU, (e) & (f) nitrate, (g) & (h) DIC, and (i) & (j) CFC-12 along transect A16S (5°S-60°S) in 2013 (left), and along transect A13.5 (5°N-55°S) in 2010 (right).

The spatial patterns of seawater properties are indicative of the large-scale water masses and their transport, and thus, they provide important context in explaining the spatial distributions of C_{anth} changes.

Salinity, AOU, nitrate, DIC, and CFC-12 were chosen to represent physical, biological and anthropogenic processes. Generally speaking, the main water property differences between transects A13.5 and A16S (Figure 2) were located in the mode and intermediate waters. Differences were also found in the deep and bottom waters (below 4000 m) in the tropical and subtropical region (north of 30°S).

A low salinity tongue originated from surface at about 45-55°S, and then transported northward centered at about 1000 m and extended to the equator. The low salinity region at the surface is indicative of the AAIW outcrop location, and the low salinity tongue represents AAIW, which is an important pathway for C_{anth} input into the ocean interior (Brewer, 1978). The fresh-water tongue in the intermediate water was more northerly along A16S than A13.5.

DIC, AOU and nitrate were higher and extended closer to the surface and further north along A13.5 than A16S, likely as a result of more accumulation of metabolic signals over slower and longer water transit time in the former. Consistent with the observed biogeochemical tracers, the CFC-12 signal was also stronger along A16S than A13.5 in the subsurface layer near the tropical region (south of 20°S).

2. Anthropogenic CO_2 Changes between 1980s and 2010s

Anthropogenic CO_2 uptake and storage increased along all three transects in the South Atlantic Ocean over the period with two common features (Figure 3). First, high ΔC_{anth} was detectable in surface and near surface waters. Second, ΔC_{anth} penetrated to deeper depths in the subantarctic and subtropical oceans and was limited to shallower depths in the tropical oceans.

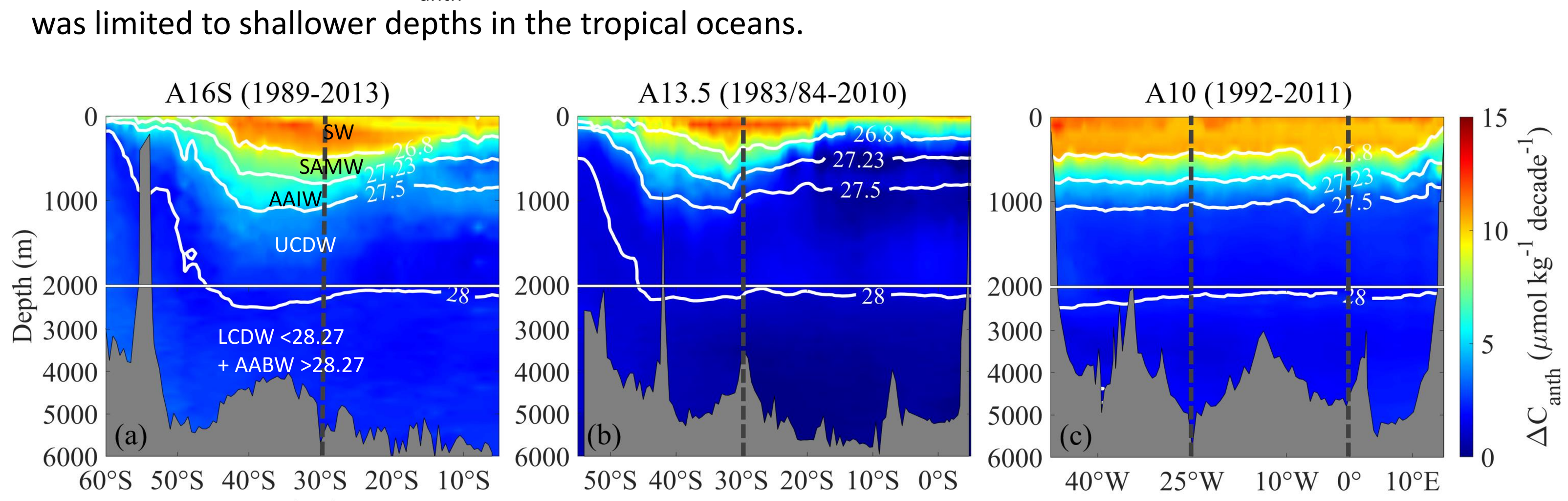

Figure 3. Anthropogenic CO_2 changes along (a) A16S (1989-2013), (b) A13.5 (1983/84-2010) and (c) A10 (1992-2011).

3. Column Inventory Changes Along Transects

Water column inventory of anthropogenic CO_2 increase is an important quantity reflecting the total amount of ΔC_{anth} in a region from both local atmospheric input and net lateral transport. Since changes in C_{anth} were mainly in the top 2000 m, here we focus on the column inventory changes in the upper 1000 m and 2000 m layers (Fig. 4). The following features emerged from this analysis: (1) ΔC_{anth} column inventory was substantially higher along the A16S than A13.5 (red vs. black lines). (2) There were clear meridional variations in the ΔC_{anth} inventory distribution with the highest water column inventory change in the subantarctic and subtropical regions. (3) Decadal ΔC_{anth} inventory increases accelerated from the 1990s to the 2000s.

The column inventory changes of C_{anth} from the 1980s to 2010s showed a similar meridional pattern for A16S and A13.5, which increased from high latitude, peaked at 30-40°S, then decreased to the equator. The mean upper 2000 m column inventory change was 0.91±0.25 mol m^{-2} yr^{-1} and 0.57±0.22 mol m^{-2} yr^{-1}, respectively, for A16S (2005-2013) and A13.5 (1983-2010). The largest west-east difference occurred at low latitudes, and then gradually decreased toward higher latitudes. For the zonal transect A10 (1992-2011), the mean column inventory change (0-2000 m) was 1.04±0.15 mol m^{-2} yr^{-1}. C_{anth} column inventory change along A10 showed only a very limited west-east contrast.

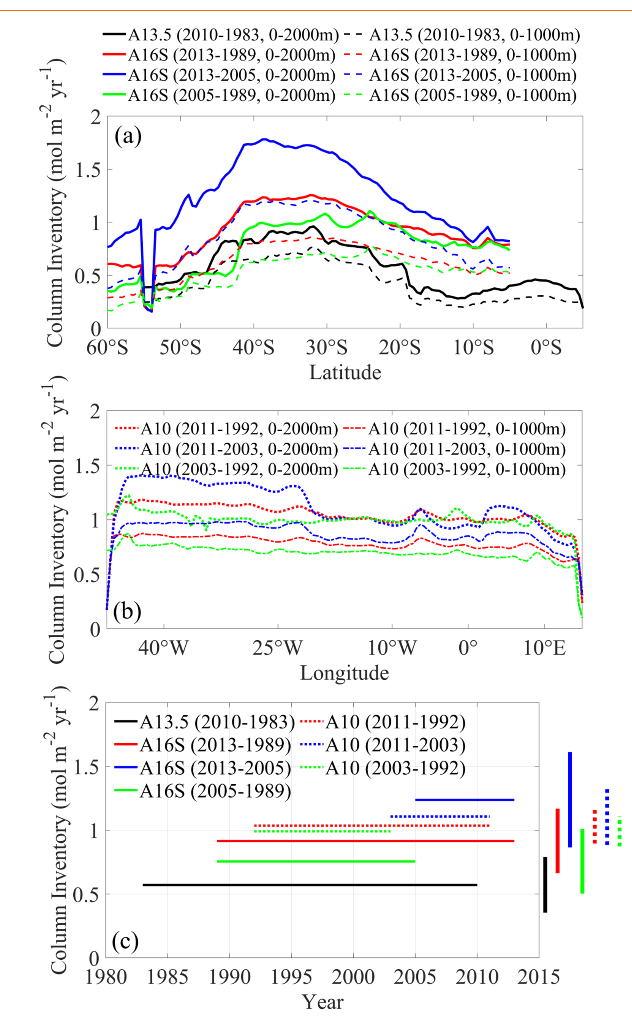

Figure 4. Column inventory change of ΔC_{anth} along (a) A16S and A13.5, (b) A10 for each time period.(c) Mean column inventory change of ΔC_{anth}, standard deviation is shown as vertical bars with matching colors along the right axes.

4. Basin-wide Total Inventory Change in the South Atlantic Ocean

Earlier, it was suggested that A16 (both the north and south transect) could be used to provide a good estimate for the entire Atlantic Ocean from the Arctic to the Antarctic (Wanninkhof et al., 2010; Talley, 2011). However, there are significant west-east DC_{anth} variability in the South Atlantic Ocean as is demonstrated here. Thus, A16S may not be representative for the entire South Atlantic Ocean. To evaluate this issue, we used both A16S (western basin) and A13.5 (eastern basin) and compared this to that using only A16S (Table 1).

The total C_{anth} uptake in the South Atlantic Ocean (0-6000 m) from the 1980s to the 2010s estimated from the sum of the western basin and eastern basin was 27% lower than that based on only A16S (3.86 vs. 5.27 Pg C $decade^{-1}$). Thus, past publications may have overestimated the total C_{anth} uptake rate based on A16S only in the South Atlantic Ocean.

Table 1. Total inventory changes of C_{anth} (Pg C $decade^{-1}$) (0-6000 m) for each 10° latitude band in the South Atlantic Ocean between 1980s and 2010s.

Latitude band	Total Inventory Change			
	West (A16S)	East (A13.5)	Summary	Use only A16S [a]
0°S - 10°S	0.40±0.01	0.16±0.002	0.56±0.01	0.87±0.02
10°S - 20°S	0.47±0.02	0.12±0.006	0.59±0.02	0.90±0.05
20°S - 30°S	0.52±0.03	0.13±0.007	0.65±0.03	1.00±0.05
30°S - 40°S	0.54±0.02	0.30±0.012	0.84±0.02	1.04±0.04
40°S - 50°S	0.63±0.03	0.21±0.034	0.84±0.04	1.03±0.05
50°S - 60°S	0.31±0.13	0.06±0.007	0.37±0.13	0.43±0.18
South Atlantic	2.87±0.14	0.99+0.03	3.86±0.14	5.27±0.20

Note. [a] In the last column, A16S-based western basin results are extrapolated to the entire South Atlantic Ocean.

Summary

1. Largest ΔC_{anth} in SW, SAMW and AAIW.
2. C_{anth} uptake rate along A16S was 2-3X of that along A13.5

--- using A16S alone would overestimate the ΔC_{anth}

3. Differences in transport and recent outcrop events were the main reasons for the ΔC_{anth} differences between the two sides of the Mid-Atlantic Ridge in the South Atlantic.

4. Wintertime export from the Weddell Sea is the main reason for the deep penetration of into the LCDW and AABW.

The latest observation in March 2020

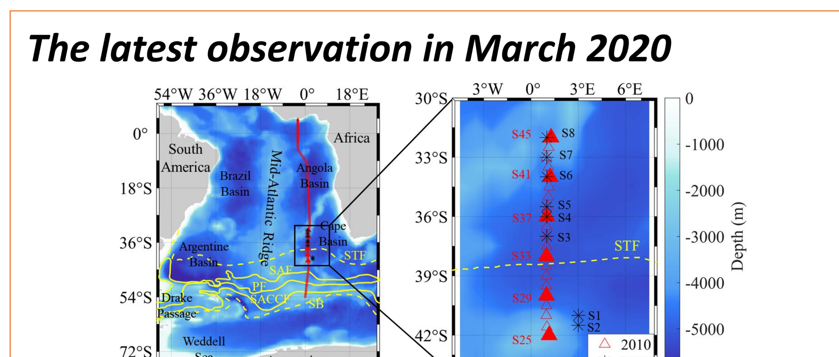

Figure 5. Map of study area and stations along A13.5 in 2010 and A12 in 2020.

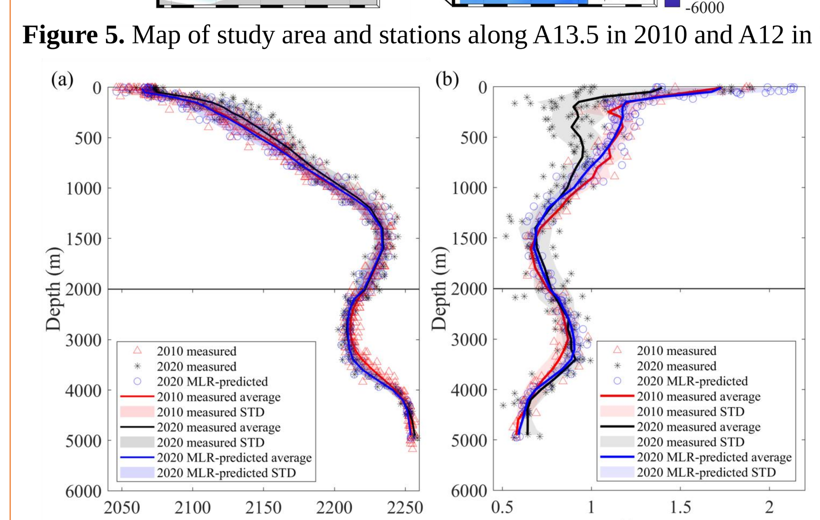

Figure 6. Vertical profiles of (a) DIC and (b) $\delta^{13}C$ measured in 2010 and 2020, and the MLR predicted DIC and $\delta^{13}C$ for 2020 in the region of 0 – 4°E and 32 – 42°S.

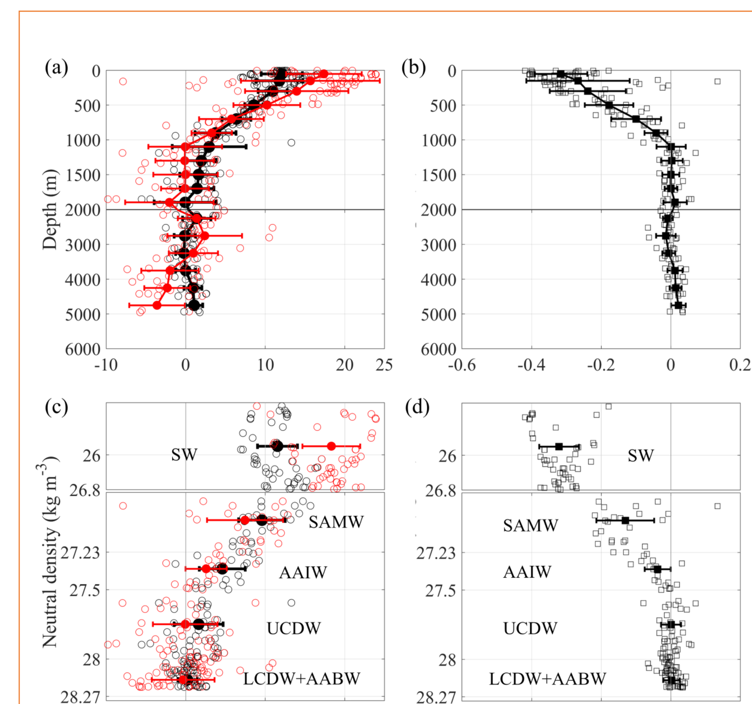

Figure 7. Depth profile of (a) anthropogenic CO_2 change estimated by DIC (black) and $\delta^{13}C$ (red, using RC values from Quay et al. (2017) & Eide et al. (2017)), (b) anthropogenic $\delta^{13}C$ change between 2010 and 2020. (c) and (d) are similar to (a) and (b) but vertically averaged within five characteristic water mass.

manuscript submitted to *Journal of Geophysical Research: Oceans*

Acknowledgement

This work was supported by the US National Science Foundation (OCE- 2123768)